Frequency tunability of solid-core photonic crystal fibers filled with nanoparticle-doped liquid crystals

Lara Scolari,[1,*] Sebastian Gauza,[2] Haiqing Xianyu,[2] Lei Zhai,[3] Lars Eskildsen,[1] Thomas Tanggaard Alkeskjold,[4] Shin–Tson Wu,[2] and Anders Bjarklev[1]

[1]*DTU Fotonik, Department of Photonics Engineering, Technical University of Denmark, Ørsteds Plads 343, DK-2800 Kgs. Lyngby, Denmark*
[2]*College of Optics and Photonics, University of Central Florida, Orlando, Florida 32816, USA*
[3]*NanoScience Technology Center, University of Central Florida, Orlando, Florida 32816, USA*
[4]*Crystal Fibre A/S, Blokken 84, 3460 Birkerød, Denmark*
[*]*Corresponding author: lsco@fotonik.dtu.dk*

Abstract: We infiltrate liquid crystals doped with $BaTiO_3$ nanoparticles in a photonic crystal fiber and compare the measured transmission spectrum with the one achieved without dopant. New interesting features, such as frequency modulation response of the device and a transmission spectrum with tunable attenuation on the short wavelength side of the widest bandgap, suggest a potential application of this device as a tunable all-in-fiber gain equalization filter with an adjustable slope. The tunability of the device is achieved by varying the amplitude and the frequency of the applied external electric field. The threshold voltage for doped and undoped liquid crystals in a silica capillary and in a glass cell are also measured as a function of the frequency of the external electric field and the achieved results are compared.

OCIS codes: (060.2310) Fiber optics; (060.5295) Photonic crystal fibers; (230.3720) Liquid-crystal devices.

References and links

1. P. St. J. Russell, "Review: Photonic Crystal Fibers," Science **299**, 358-362 (2003).
2. A. Bjarklev, J. Broeng, and A. S. Bjarklev, *Photonic Crystal Fibres* (Kluwer Academic, Dordrecht, 2003).
3. N. M. Litchinitser, S. C. Dunn, P. E. Steinvurzel, B. J. Eggleton, T. P. White, R. C. McPhedran, and C. M. de Sterke, "Application of an ARROW model for designing tunable photonic devices," Opt. Express **12,** 1540–1550 (2004).
4. B. J. Eggleton, C. Kerbage, P. S. Westbrook, R. S. Windeler, and A. Hale, "Microstructured Optical Fiber Devices," Opt. Express **9,** 698–713 (2001).
5. C. Kerbage, R. S. Windeler, B. J. Eggleton, P. Mach, M. Dolinski, and J. A. Rogers, "Tunable devices based on dynamic positioning of micro-fluids in micro-structured optical fiber," Opt. Commun. **204,** 179–184 (2002).
6. R. T. Bise, R. S.Windeler, K. S. Kranz, C. Kerbage, B. J. Eggleton, and D. J. Trevor, "Tunable photonic band gap fiber," Optical Fiber Communication Conference, 466–468 (2002).
7. S. Gauza, C. H. Wen, S. T. Wu, N. Janarthanan, and C. S. Hsu, "Super high birefringence isothiocyanato biphenyl-bistolane liquid crystals," Jpn. J. Appl. Phys. **43**, 7634-7638 (2004).
8. S. T. Wu, Q. T. Zhang, and S. Marder, "High dielectric dopants for low voltage liquid crystal operation," Jpn. J. Appl. Phys. **37**, L1254-L1256 (1998).
9. T. T. Larsen, A. Bjarklev, D. S. Hermann, and J. Broeng, "Optical devices based on liquid crystal photonic bandgap fibres," Opt. Express **11,** 2589–2596 (2003).
10. M.W. Haakestad, T. T. Alkeskjold, M. D. Nielsen, L. Scolari, J. Riishede, H. E. Engan, and A. Bjarklev, "Electrically tunable photonic bandgap guidance in a liquid-crystal-filled photonic crystal fiber," IEEE Photon. Technol. Lett. **17,** 819–821 (2005).
11. L. Scolari, T. T. Alkeskjold, J. Riishede, A. Bjarklev, D. Hermann, A. Anawati, M. Nielsen, and P. Bassi, "Continuously tunable devices based on electrical control of dual-frequency liquid crystal filled photonic bandgap fibers," Opt. Express **13,** 7483–7496 (2005).

#106776 - $15.00 USD Received 23 Jan 2009; revised 21 Feb 2009; accepted 23 Feb 2009; published 25 Feb 2009

12. F. Du, Y. Q. Lu, and S. T. Wu, "Electrically tunable liquid-crystal photonic crystal fiber," Appl. Phys. Lett. **85**, 2181–2183 (2004).
13. T. T. Alkeskjold, J. Lægsgaard, A. Bjarklev, D. Hermann, A. Anawati, J. Broeng, J. Li, and S. T. Wu, "All-optical modulation in dye-doped nematic liquid crystal photonic bandgap fibers," Opt. Express **12,** 5857–5871 (2004).
14. L. Scolari, T. T. Alkeskjold, and A. Bjarklev, "Tunable Gaussian filter based on tapered liquid crystal photonic bandgap fibre," Electron. Lett. **42,** 1270–1271 (2006).
15. D. Noordegraaf, L. Scolari, J. Lægsgaard, L. Rindorf, and T. T. Alkeskjold, "Electrically and mechanically induced long period gratings in liquid crystal photonic bandgap fibers," Opt. Express **15**, 7901-7912 (2007).
16. D. Noordegraaf, L. Scolari, J. Lægsgaard, T. T. Alkeskjold, G. Tartarini, E. Borelli, P. Bassi, J. Li, and S. T. Wu, "Avoided-crossing-based liquid-crystal photonic-bandgap notch filter," Opt. Lett. **33,** 986–988 (2008).
17. T. R. Wolinski, S. Ertman, P. Lesiak, A. W. Domanski, A. Czapla, R. Dabrowski, E. Nowinowski-Kruszelnicki, and J. Wojcik, "Photonic liquid crystal fibers - a new challenge for fiber optics and liquid crystals photonics," Opto-Electronics Review **14,** 329–334, (2006).
18. T. R. Wolinski, A. Czapla, S. Ertman, M. Tefelska, A. W. Domanski, E. Nowinowski-Kruszelnicki, and R. Dabrowski, "Tunable highly birefringent solid-core photonic liquid crystal fibers," Opt. Quantum Electron. **39,** 1021–1032 (2007).
19. T. R. Wolinski, S. Ertman, A. Czapla, P. Lesiak, K. Nowecka, A. W. Domanski, E. Nowinowski-Kruszelnicki, R. Dabrowski, and J.Wojcik, "Polarization effects in photonic liquid crystal fibers," Meas. Sci. Technol. **18,** 3061–3069 (2007).
20. D. C. Zografopoulos, E. E. Kriezis, and T. D. Tsiboukis, "Tunable highly birefringent bandgap-guiding liquid crystal microstructured fibers," J. Lightwave Techol. **24,** 3427–3432 (2006).
21. C. J. Kiely, J. Fink, M. Brust, D. Bethell, and D. J. Schiffrin, "Spontaneous ordering of bimodal ensembles of nanoscopic gold nanoparticles," Nature **396**, 444-446 (1998).
22. J. S. Bradley, "Clusters and Colloids: From Theory and Application," edited by G. Schmid, VCH, Weinheim, (1994).
23. S. Kundu, M. Akimoto, I. Hirayama, M. Inoue, S. Kobayashi, and K. Takatoh, "Enhancement of contrast ratio by using ferroelectric nanoparticles in the alignment layer of liquid crystal display," Jpn. J. Appl. Phys. **47**, 4751-4754 (2008).
24. M. Kaczmarek, O. Buchnev, and I. Nandhakumar, "Ferroelectric nanoparticles in low refractive index liquid crystals for strong electro-optic response," Appl. Phys. Lett. **92**, 103307 (2008).
25. S. Kobayashi, T. Miyama, N. Nishida, Y. Sakai, H. Shiraki, Y. Shiraishi, and N. Toshima, "Dielectric spectroscopy of metal nanoparticle doped liquid crystal displays exhibiting frequency modulation response," J. Display Technology **2**, 121-129 (2006).
26. Y. Shiraishi, N. Toshima, K. Maeda, H. Yoshikawa, J. Xu, and S. Kobayashi, "Frequency modulation response of a liquid-crystal electro-optic device doped with nanoparticles," App. Phys. Lett. **81**, 147801, (2006).
27. Y. Reznikov, O. Buchnev, O. Tereshchenko,V. Reshetnyak, A. Glushchenko, and J. West, "Ferroelectric nematic suspension," Appl. Phys. Lett. **82**, 1917-1919, (2003).
28. F. Li, O. Buchnev, C. I. Cheon, A. Glushchenko, V. Reshetnyak, Y. Reznikov, T. J. Sluckin and J. L. West, "Orientational coupling amplification in ferroelectric nematic colloids," Phys. Rev. Lett. **97**, 147801, (2006).
29. V. G. Chigrinov, *Liquid Crystal Devices* (Artech-House, 1999).
30. S. Gauza, H. Wang, C. H. Wen, S. T. Wu, A. Seed, and R. Dabrowski, "High birefringence isothiocyanato tolane liquid crystals," Jpn. J. Appl. Phys. Part 1 **42**, 3463-3466 (2003).
31. S. T. Wu, U. Efron, and L. D. Hess, "Birefringence measurements of liquid crystals," Appl. Opt. **23**, 3911-3915 (1984). .

1. Introduction

Photonic crystal fibers (PCFs) have attracted significant attention in the last decade because of their new properties [1,2] and the many interesting applications they can lead to. The microstructure allows the realization of either the so-called high-index guiding fibers, which guide light in a high-index core similarly to the total internal reflection principle, or the so-called bandgap-guiding fibers, which guide light in a low-index core by means of coherent reflections from the surrounding periodic structure [3]. Furthermore, the presence of air holes in the structure gives the possibility to infuse liquids and, therefore, to create tunable devices [4-6]. Among liquid materials, liquid crystals represent a very good candidate for the fabrication of tunable all-in-fiber components because they exhibit very high electro-optic and thermo-optic effects due to high birefringence ($\Delta n \sim 0.8$) [7] and large dielectric anisotropy ($\Delta \varepsilon \sim 70$) [8]. If typical index-guiding PCFs are infiltrated with liquid crystals, they start

#106776 - $15.00 USD Received 23 Jan 2009; revised 21 Feb 2009; accepted 23 Feb 2009; published 25 Feb 2009

guiding light by the bandgap effect, since liquid crystals have refractive indices higher than that of silica. Based on liquid crystal filled PCFs (LCPCF), devices which can be thermally, electrically or optically tuned, have been demonstrated [9-20]. Among these, we find, for example, devices for tuning, scrambling and controlling the polarization [11,19] tunable Gaussian filters for Optical Coherence Tomography (OCT) [14], tunable electrically and mechanically induced gratings [15], tunable notch filters [16], devices with tunable birefringence [18] and devices for single-polarization and high-birefringence guidance [20].

In the last decade, considerable research has been devoted to fabrication and study of nanomaterials [21,22] that can be used for electro-optic device technology such as liquid crystal displays. Ferroelectric or metal nanoparticles can be dispersed, for example, in the alignment layer in order to orient liquid crystal molecules and increase the contrast ratio [23] or can also be directly dispersed in the liquid crystal matrix in order to increase birefringence and dielectric anisotropy [24] or induce frequency modulation response [25,26].

In this paper, for the first time to our knowledge, we measure and discuss the characteristics of a photonic crystal fiber infiltrated with liquid crystals doped with barium titanate ($BaTiO_3$) nanoparticles. The frequency dependent behavior of the nanoparticles influences the frequency dependent behavior of the liquid crystal in which they are dispersed, resulting in the possibility of tuning the transmission spectrum by varying the frequency of the applied electric field. Furthermore, the fabricated device presented here has a transmission spectrum with an interesting feature on the short wavelength side of the bandgap edge. For voltages below 160 V_{rms}, in fact, only the short wavelength side of the bandgap is influenced by the application of an external field and the slope of this edge is adjustable by changing frequency and amplitude of the applied voltage. This characteristic makes the device particularly attractive as a telecommunication device and, in particular, as a tunable all-in-fiber gain equalization filter. The voltage threshold and its frequency dependent behavior are also measured and compared for both undoped and doped liquid crystals infiltrated in a silica capillary and, successively, in a glass cell.

2. Preparation of the device

In this experiment, we used a high-index core PCF named LMA-10 (Crystal Fibre A/S, Denmark) with a core surrounded by 7 rings of air holes arranged in a triangular lattice (Fig. 1 (a)). The hole diameter is 3.1 μm, the inter-hole distance is 7.2 μm and the cladding diameter is 125 μm. The mixture used to infiltrate the fiber is a liquid crystal, E7 (Merck, Darmstadt, Germany), in which $BaTiO_3$ nanoparticles are dispersed. The measured dielectric anisotropy $\Delta\varepsilon$ of this mixture at 1 kHz is 13.4, the splay elastic constant K_{11} is 7.34 pN and the bend elastic constant K_{33} is 9.3 pN. $BaTiO_3$ nanoparticle dispersion in E7 was prepared as follows: 50 mg of nanoparticles were suspended in 20 mL of dimethyl sulfoxide (DMSO) together with 50 mg of a pentylcyanobiphenyl (5CB) liquid crystal as a dispersant by sonification for 4 hours. 0.25 mL of this suspension was added to 1 g of E7 using sonification for 1 hour. Then the mixture was held under vacuum (0.1 torr) for 48 hours in order to remove the DMSO. The final concentration of nanoparticles was estimated to be around 0.01% by weight. The problem of mixture stability is a sensitive topic and was reported by several research groups. In [27], for example, a liquid crystal mixture with $Sn_2P_2S_6$ nanoparticles was found to be stable for at least 6 months and in [28] a liquid crystal mixture with $BaTiO_3$ nanoparticles was found to be stable for at least one year. In case of our experiment, sedimentation of nanoparticles was observed during the first step of the dispersing process. Therefore, the concentration of the nanoparticles in the liquid crystal host was further decreased until no sedimentation was observed. The experiments with infiltrated fiber were repeated after 3 months and showed the same results. We infiltrated the fiber with this mixture for 14 mm of its length by using capillary forces. Polarized optical microscopy observations of a 5-μm silica capillary tube infiltrated with this mixture indicates that the liquid crystal directors exhibit planar alignment along the axis of the fiber, similarly to pure E7 [13]. Figure 1(b) shows a polarized micrograph of this mixture when the capillary is oriented at 45 degrees with respect

#106776 - $15.00 USD Received 23 Jan 2009; revised 21 Feb 2009; accepted 23 Feb 2009; published 25 Feb 2009

to the crossed polarizers. Since the alignment is planar we used the same procedure that we applied to pure E7 [13] in order to stabilize the molecular alignment: we heated the mixture up to the isotropic phase and then cooled it down slowly. Then, we positioned the fiber on a xyz Thorlabs stage equipped with a thermal plate and electrodes. The transmission of the fiber device was measured using a white light from a Tungsten-Halogen light source as shown in Fig. 2. Light from the source was guided by a LMA fiber and coupled into the LCPCF fiber by aligning the two fibers on the xyz-stage. The liquid crystal mixture did not leak out from the fiber since no pressure was applied to the holes of the fiber. Capillary forces keep the LC about 200-300 μm far from the end-facet of the fiber. The transmission was then measured by an optical spectrum analyzer (ANDO, AQ6317B) and normalized to that of the unfilled fiber. Later, in order to apply an external electric field to the device, we added to the setup a function generator (Tektronics, AFG 3101) and an amplifier (Krohn-hite, 7500).

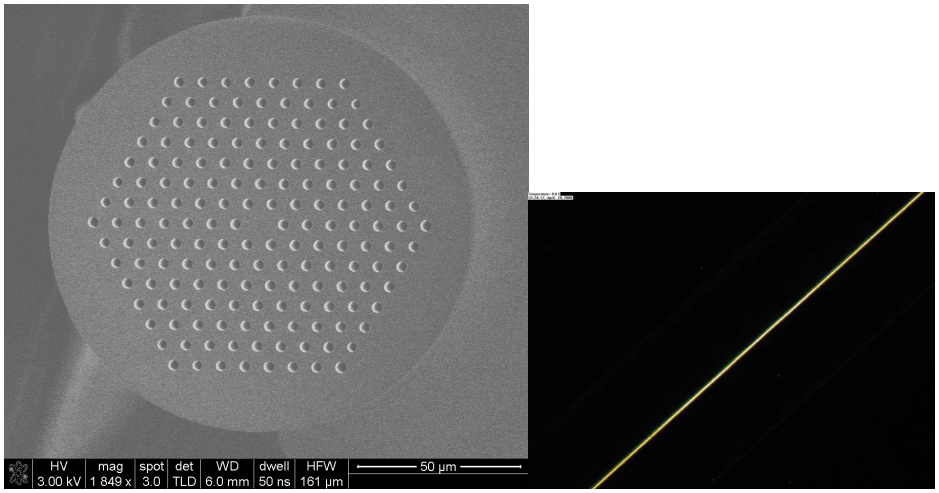

(a) (b)

Fig. 1. (a) SEM image of the PCF end facet. (b) Polarization optical micrograph of a 5 μm silica capillary infiltrated with E7 doped with $BaTiO_3$ nanoparticles.

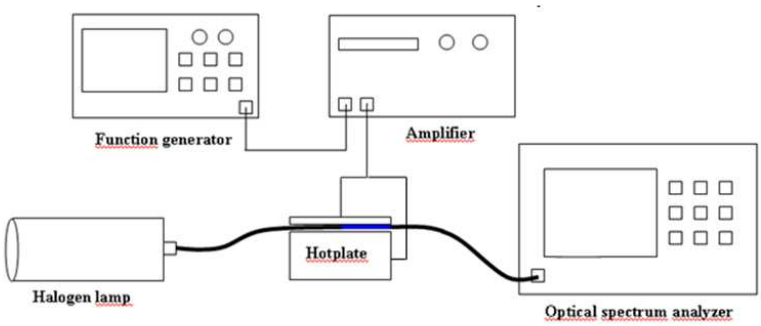

Fig. 2. Setup used to measure the transmission spectrum of the fabricated device.

#106776 - $15.00 USD Received 23 Jan 2009; revised 21 Feb 2009; accepted 23 Feb 2009; published 25 Feb 2009

3. Spectral properties and frequency tunability

We measured the transmission spectrum first, without applying any external electric field. Figure 3 shows the transmission spectrum at three different temperatures. The loss in the middle of the widest bandgap is 1.5 dB, comparable to the one achieved with undoped E7 [13], indicating that the presence of nanoparticles does not induce extra scattering and, therefore, any extra loss. Also the thermal tunability is comparable to pure E7 [13].

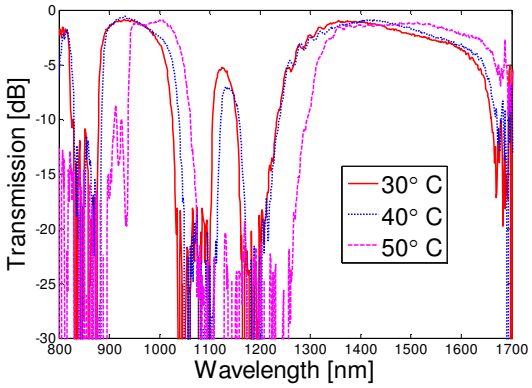

Fig. 3. Transmission spectrum of LMA-10 infiltrated with E7 doped with $BaTiO_3$ nanoparticles at three different temperatures.

In order to investigate the frequency dependence induced by the nanoparticles we applied to the infiltrated section a sinusoidal voltage at different frequencies (100 Hz, 500 Hz, 1 kHz, 10 kHz, 30 kHz and 100 kHz) and we recorded the transmission spectrum for each frequency. For each frequency we also varied the amplitude of the voltage from 0 to 200 V_{rms} in steps of 40 V_{rms}. In order to study the effect of the nanoparticles added to the liquid crystals, we carried out the same measurements for pure E7 and compare the two results. Figure 4 shows various transmission spectra of the PCF filled with nanoparticle-doped E7 (Figs. 4(a), (b) and (c) at 100 Hz, 500 Hz and 1 kHz, respectively) and with pure E7 (Figs. 4(d), (e) and (f) at 100 Hz, 500 Hz and 1 kHz, respectively). We note that, while the behaviour of E7 is not affected by the frequency of the applied field, the behaviour of E7 doped with nanoparticles is strongly influenced by the frequency chosen. In particular, we can observe from Figs. 4(a) and 4(d) that, for example at 100 Hz, there is almost no change of the bandgaps for the nanoparticle-doped E7 with a voltage in the range 0-200 V_{rms}, while pure E7 responds at the same frequency if a voltage > 100 V_{rms} is applied. By stepwise increasing the frequency of the ac field, we notice that the intensity of the response to the field increases towards 1 kHz to become lower again at 100 kHz (see Fig. 5). In fact, while the E7 response is almost the same in the range 100 Hz-100 kHz, this does not apply to E7 doped with $BaTiO_3$ nanoparticles. In this case, at high frequencies the response is lower because the nanoparticles cannot follow the ac field, therefore 'blocking' also the reorientation of the liquid crystal molecules in contact with the nanoparticles. For the low frequency case, the ionic impurities that might exist in the E7 host or have been introduced during dispersion of nanoparticles can cause shielding of the low frequency field. Therefore, in both cases, a higher voltage with respect to pure E7 is needed to observe a change of the bandgaps.

#106776 - $15.00 USD Received 23 Jan 2009; revised 21 Feb 2009; accepted 23 Feb 2009; published 25 Feb 2009

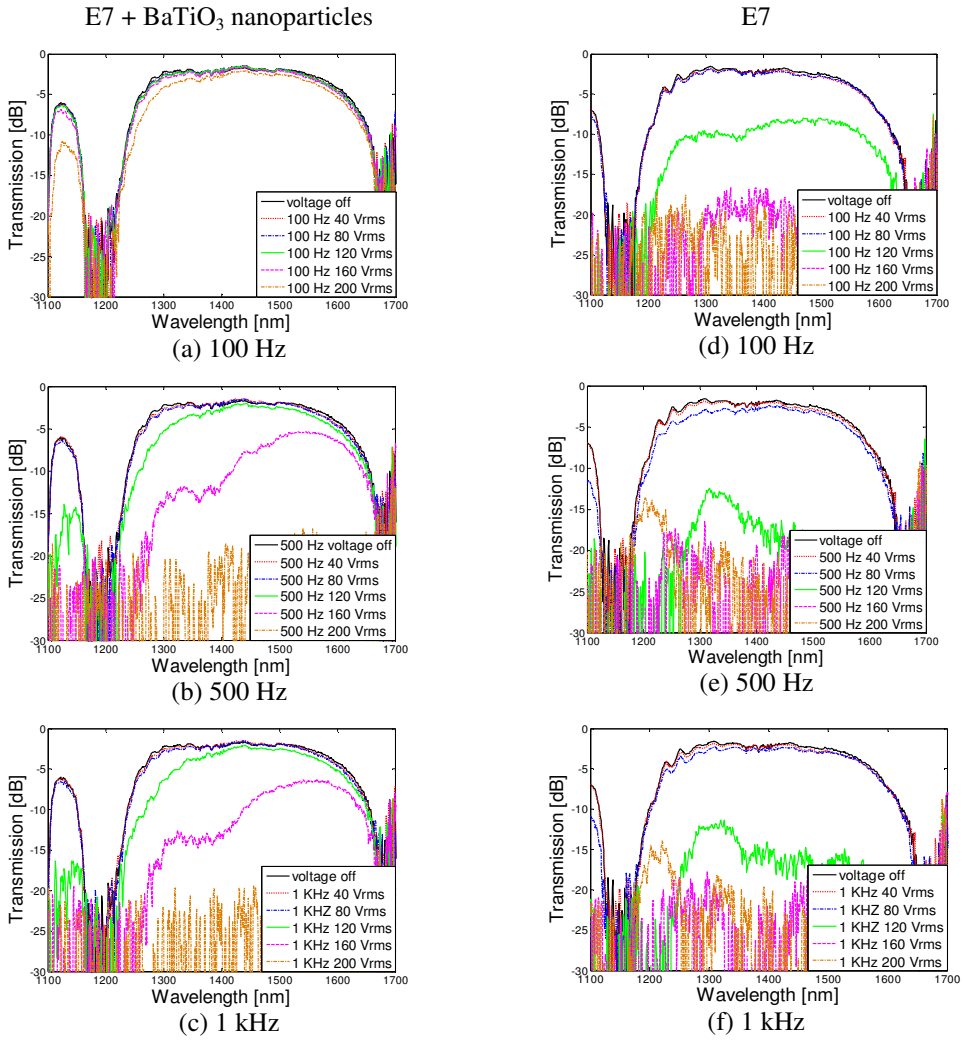

Fig. 4. Transmission spectrum at various frequencies and amplitudes of the external electric field for LMA-10 infiltrated nanoparticle-doped E7 ((a), (b) and (c)) and for LMA-10 infiltrated with pure E7 ((d), (e) and (f)).

Another interesting characteristic of the transmission spectrum of LMA-10 infiltrated with nanoparticle-doped E7 is that, for voltages below 160 V_{rms}, only the short wavelength side of the bandgap is influenced by the application of an external field. In the case of nanoparticle-doped E7 it seems that the EH_{11} mode (which determines the short bandgap edge) is pushed more into the bandgap with respect to the pure E7 case. Figure 5 shows this effect, together with the bandgap frequency tunability. We note that the effect of the field is only on the short side of the bandgap and that its slope can be adjusted by varying the frequency of the applied field. This effect can be potentially used as a gain equalization filter or as a tunable filter which can be dynamically adjusted to meet the requirement of the network.

#106776 - $15.00 USD Received 23 Jan 2009; revised 21 Feb 2009; accepted 23 Feb 2009; published 25 Feb 2009

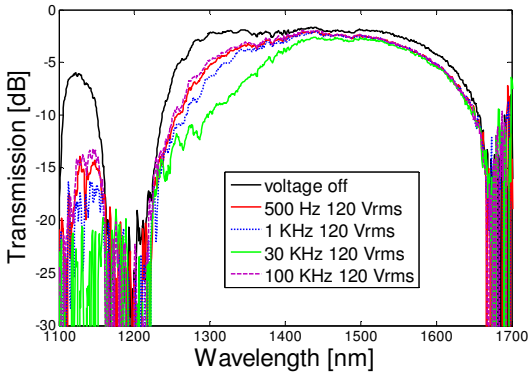

Fig. 5. Transmission spectrum of LMA-10 infiltrated with nanoparticle-doped E7 as a function of the frequency of the external electric field. The amplitude of the voltage here is constant (120 V_{rms}). The shape of the short wavelength edge can be controlled through adjustment of the frequency.

4. Threshold voltage for capillary geometry

We also studied liquid crystal alignment under the effect of an external electric field using a polarized optical microscope. This allowed us to measure the threshold voltage at different frequencies and have a further proof of what we observed in a PCF in the previous section. A silica capillary tube with an inner diameter of 5 μm and an outer diameter of 150 μm was filled first with the nanoparticle-doped E7 mixture and afterwards with pure E7. The capillary was sandwiched between two glass plates covered with transparent indium-tin-oxide (ITO); two unfilled capillaries were used as spacers and a few drops of a UV-curable polymer on the electrodes made sure that the filled capillary did not move while under study. Polarized optical microscopy is a standard procedure used in order to investigate the alignment of liquid crystals [9-13]; by increasing the amplitude of the applied ac field, the liquid crystal realigns and a change of color can be observed through the microscope. For planar aligned liquid crystals, their molecules move only if the amplitude of the voltage is above a certain threshold, called the Frederiks transition [29]. As the voltage increases, the first change of color corresponds to the Frederiks transition threshold (see Fig. 6). We also varied the frequency of the ac field and we repeated the same procedure in order to have the threshold for each frequency chosen. We find that the threshold is higher than that of pure E7 at low frequencies (100 Hz and 500 Hz), comparable with E7 at 1 kHz, 30 kHz and 50 kHz and increases again towards 100 kHz. This is in agreement with the transmission spectrum discussed in Figs. 4 and 5. Pure E7, on the other hand, is not strongly influenced by the frequency of the applied field, in accordance with the observations in Fig. 4. Figure 7 shows the measured Frederiks transition for both pure E7 and nanoparticle-doped E7 as a function of the frequency of the external field.

#106776 - $15.00 USD Received 23 Jan 2009; revised 21 Feb 2009; accepted 23 Feb 2009; published 25 Feb 2009

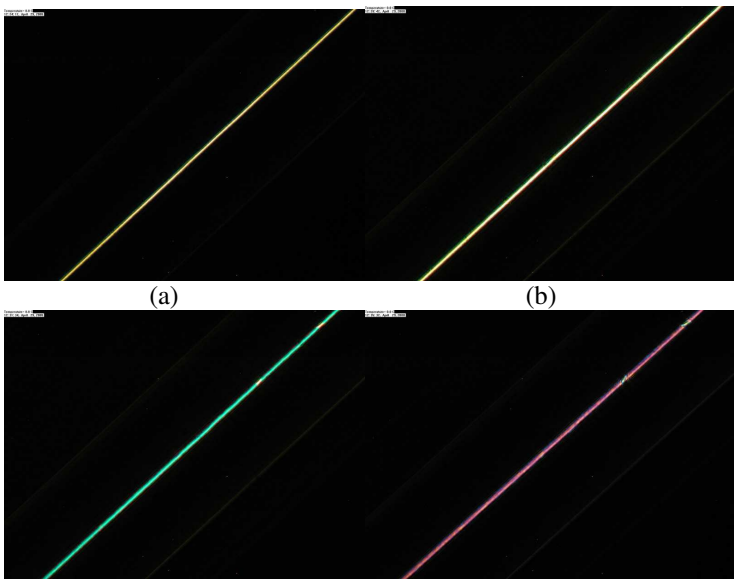

Fig. 6. Polarization optical micrograph of a 5 μm silica capillary infiltrated with nanoparticle-doped E7 for (a) V=0V_{rms}, f=1kHz, (b) V=62V_{rms}, f=1kHz, (c) V=88V_{rms}, f=1kHz, (d) V=116V_{rms}, f=1kHz.

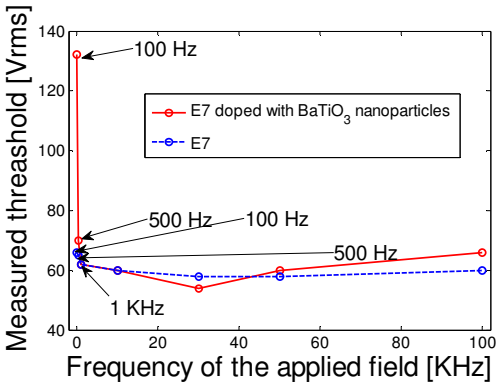

Fig. 7. Measured Frederiks threshold at different frequencies for nanoparticles-doped E7 and pure E7 in a silica capillay.

5. Threshold voltage for cell geometry

We also measured the threshold voltage of both doped and undoped E7 in a glass cell, again in order to have a further proof of what we observed inside a PCF. In fact, we expect the frequency dependent behavior to appear also in the case of a cell. We prepared a homogeneous cell, i.e. with planar alignment layer, with a cell gap d~8 μm and we filled it with nanoparticle-doped E7. Later, we did the same experiment, but with pure E7. Figure 8 shows the schematic diagrams of the experimental setup. A He-Ne laser (λ=632.8nm) was used as light source. The linear polarizer was oriented at 45º with respect to the liquid crystal rubbing direction and the analyzer was crossed. This configuration gives the maximum phase retardation of the linearly polarized light impinging upon the cell, due to different propagating speed of the extraordinary and ordinary rays in the liquid crystal medium. The phase retardation (δ) is expressed as [30,31]:

#106776 - $15.00 USD Received 23 Jan 2009; revised 21 Feb 2009; accepted 23 Feb 2009; published 25 Feb 2009

$$\delta(V,T,\lambda) = 2\pi d\Delta n(V,T,\lambda)/\lambda \quad (1)$$

where d is the cell thickness, Δn is the effective liquid crystal birefringence, T the temperature and λ the wavelength. The normalized transmittance is related to δ as following [30,31]:

$$T = \sin^2(\delta/2) \quad (2)$$

The transmission was measured by a photodiode detector (New Focus Model 2031) and recorded digitally by a data acquisition system (DAQ, PCI 6110) using LabVIEW. An AC voltage square wave was used to drive the liquid crystal cell whose inner sides were coated with ITO electrodes. On top of the ITO, the substrate was covered with a thin polyimide alignment film. The buffing induced pretilt angle is about 3°. The transmission was measured at various frequencies of the ac field. In our experiments, we found that the square shape of the signal was undistorted by the amplifier only for frequencies in the range 10 Hz-10 kHz, therefore we conducted measurements only in this range (at 10 Hz, 50 Hz, 100 Hz, 500 Hz, 1 kHz, 10 kHz). We carried our planar cell experiment at elevated temperature of 40°C. The threshold voltage change upon frequency was more obvious at elevated temperature than if we had conducted the same experiment at regular room temperature conditions. We explain this phenomenon based on decreased rotational viscosity which will make E7 liquid crystal molecules more vulnerable to be affected by driving voltage frequency change.

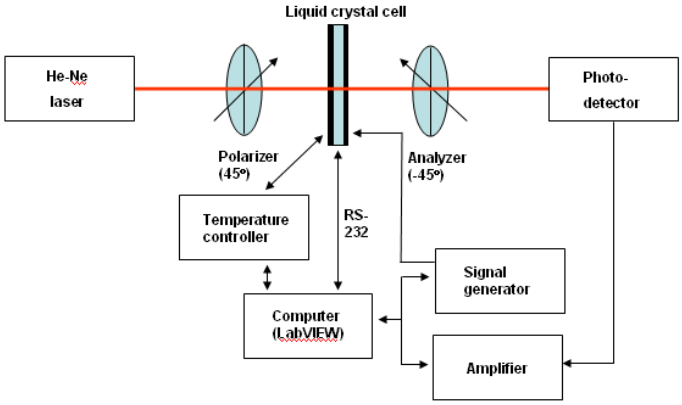

Fig. 8. Experimental setup for measuring the threshold voltage of a glass cell infiltrated with liquid crystal.

The recorded transmissions of the doped liquid crystal cell for different frequencies of the applied electric field (10 Hz, 100 Hz 500 Hz, 10 kHz) are shown in Fig. 9.

It is now possible to calculate δ by inverting formula (2). In order to calculate the threshold voltage, we plot the phase change $\Delta\phi = \delta_{max}-\delta$ as a function of voltage and we do a linear extrapolation near the threshold region [31], as shown in Fig. 10.

#106776 - $15.00 USD Received 23 Jan 2009; revised 21 Feb 2009; accepted 23 Feb 2009; published 25 Feb 2009

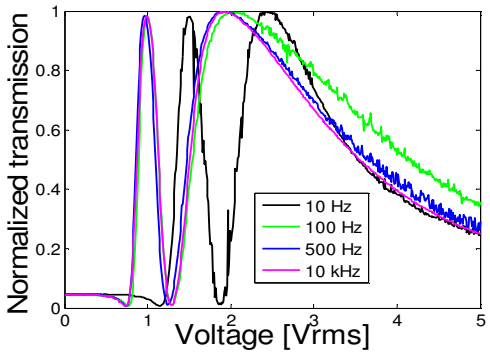

Fig. 9. Voltage-dependent transmission of a homogeneous 8-μm cell filled with $BaTiO_3$ nanoparticle-doped E7 for different frequencies of the external applied field.

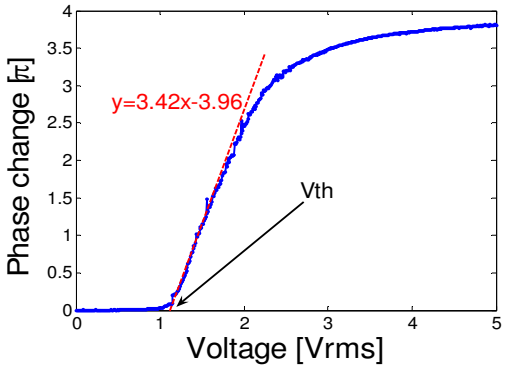

Fig. 10. Voltage-dependent phase change of the $BaTiO_3$ nanoparticle-doped cell when a 10 Hz square wave is applied to the cell. The phase change is linear with the voltage near the threshold region [31]. The threshold voltage V_{th} is, in this case extrapolated to be equal to 1.15 V_{rms}.

We calculate the phase change and the threshold voltage for 10 Hz, 50 Hz, 100 Hz, 500 Hz, 1 kHz and 10 kHz. Figure 11 shows the threshold voltage as a function of frequency for both doped and undoped E7. Again we find a similar behavior for the threshold voltage as a function of frequency (low frequency case) as the one we found before for a capillary. Unfortunately, we were not able to explore the high frequency case, because of limitation of the setup used, as explained above.

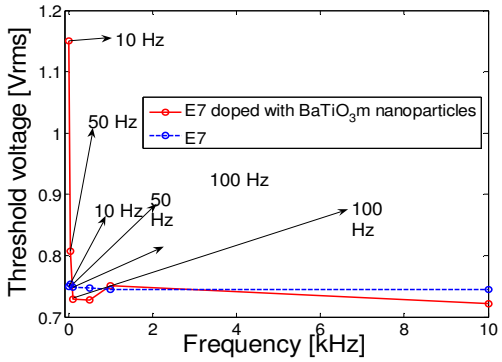

Fig. 11. Measured Frederiks transition threshold at different frequencies for nanoparticle-doped E7 and pure E7 in a glass cell.

#106776 - $15.00 USD Received 23 Jan 2009; revised 21 Feb 2009; accepted 23 Feb 2009; published 25 Feb 2009

6. Conclusions

We have fabricated a device based on a photonic crystal fiber infiltrated with liquid crystals doped with $BaTiO_3$ nanoparticles. Compared to similar devices based on undoped liquid crystal, new interesting features appears, such as a frequency modulation response and a transmission spectrum with tunable attenuation on the short wavelength side of the bandgap. This suggests a potential application of this device as a tunable all-in-fiber gain equalization filter with an adjustable slope. The frequency dependence of the $BaTiO_3$ nanoparticle- doped liquid crystal mixture has also been investigated in a silica capillary and in a glass cell and shows an analogous behavior to the one observed in a PCF.

#106776 - $15.00 USD Received 23 Jan 2009; revised 21 Feb 2009; accepted 23 Feb 2009; published 25 Feb 2009